2005

Impact of highly basic solutions on sorption of Cs+ to subsurface sediments from the Hanford site, USA

C.C. Ainsworth
Pacific Northwest National Laboratory, calvin.ainsworth@pnl.gov

John M. Zachara
Pacific Northwest National Laboratory, john.zachara@pnl.gov

K. Wagnon
Pacific Northwest National Laboratory

S. McKinley
Pacific Northwest National Laboratory

Chongxuan Liu
Pacific Northwest National Laboratory, chongxuan.liu@pnl.gov

See next page for additional authors

Geochimica et Cosmochimica Acta, Vol. 69, No. 20, pp. 4787–4800, 2005

0016-7037/05 $30.00 + .00

doi:10.1016/j.gca.2005.06.007

Impact of highly basic solutions on sorption of Cs^+ to subsurface sediments from the Hanford site, USA

C. C. Ainsworth,* J. M. Zachara, K. Wagnon, S. McKinley, C. Liu, S. C. Smith, H. T. Schaef, and P. L. Gassman
Pacific Northwest National Laboratory, MSIN P7-54, P.O. Box 999, Richland, WA USA

(*Received June* 18, 2004; *accepted in revised form June* 14, 2005)

Abstract—The effect of caustic $NaNO_3$ solutions on the sorption of ^{137}Cs to a Hanford site micaceous subsurface sediment was investigated as a function of base exposure time (up to 168 d), temperature (10°C or 50°C), and NaOH concentration (0.1 mol/L to 3 mol/L). At 10°C and 0.1 M NaOH, the slow evolution of $[Al]_{aq}$ was in stark contrast to the rapid increase and subsequent loss of $[Al]_{aq}$ observed at 50°C (regardless of base concentration). Exposure to 0.1 M NaOH at 10°C for up to 168 d exhibited little if any measurable effect on sediment mineralogy, Cs^+ sorption, or Cs^+ selectivity; sorption was well described with a two-site ion exchange model modified to include enthalpy effects. At 50°C, dissolution of phyllosilicate minerals increased with [OH]. A zeolite (tetranatrolite; $Na_2Al_2Si_3O_{10}{\cdot}2H_2O$) precipitated in 0.1 M NaOH after about 7 days, while an unnamed mineral phase ($Na_{14}Al_{12}Si_{13}O_{51}{\cdot}6H_2O$) precipitated after 4 and 2 days of exposure to 1 M and 3 M NaOH solutions, respectively. Short-term (16 h) Cs^+ sorption isotherms (10^{-9}–10^{-2} mol/L) were measured on sediment after exposure to 0.1 M NaOH for 56, 112, and 168 days at 50°C. There was a trend toward slightly lower conditional equilibrium exchange constants ($\Delta\log {}^{Cs}_{Na}K_c \sim 0.25$) over the entire range of surface coverage, and a slight loss of high affinity sites (15%) after 168 days of pretreatment with 0.1 M base solution. Cs^+ sorption to sediment over longer times was also measured at 50°C in the presence of NaOH (0.1 M, 1 M, and 3 M NaOH) at Cs^+ concentrations selected to probe a range of adsorption densities. Model simulations of Cs^+ sorption to the sediment in the presence of 0.1 M NaOH for 112 days slightly under-predicted sorption at the lower Cs^+ adsorption densities. At the higher adsorption densities, model simulations under-predicted sorption by 57%. This under-prediction was surmised to be the result of tetranatrolite precipitation, and subsequent slow Na → Cs exchange. At higher OH concentrations, Cs^+ sorption in the presence of base for 112 days was unexpectedly equal to, or greater than that expected for pristine sediment. The precipitation of secondary phases, coupled with the fairly unique mica distribution and quantity across all size-fractions in the Hanford sediment, appears to mitigate the impact of base dissolution on Cs^+ sorption. *Copyright © 2005 Elsevier Ltd*

1. INTRODUCTION

The extraction of Pu and other strategic materials from irradiated uranium fuels generates large volumes of high-level nuclear waste (HLW). A major component of the Pu reprocessing waste is ^{137}Cs, a high yield fission product ($t_{1/2}$ = 37.5 yr), that is of environmental concern because of its high-energy gamma emission. In the United States, HLW is stored at DOE facilities including Hanford, Idaho National Engineering Laboratory, and Savannah River in massive underground tanks. At the Hanford site, large concentrations of ^{137}Cs-containing HLW has been released to the vadose zone and discharged to the soil surface. ^{137}Cs migration through the micaceous Hanford sediments, under normal conditions is limited. However, concerns exist that the highly alkaline and saline nature of these wastes might decrease sediment sorptivity and expedite ^{137}Cs migration.

Previously, Zachara et al. (2002) demonstrated that ion exchange controlled Cs^+ sorption to the Hanford sediment, whose layer aluminosilicate minerals selectively sorbed Cs^+ over other monovalent cations. Similar Cs^+ behavior has been observed in soils, and sediments by others (Francis and Brinkley, 1976; Evans et al., 1983; Maes and Cremers, 1986; Cremers et al., 1988; Grütter et al., 1990; Wauters et al., 1996a, 1996b; Chitra et al., 1999). Hanford sediment Cs^+ exchange was well described by a two site ion exchange model (Zachara et al., 2002), which incorporated the sites existing along the frayed edges of micaeous minerals [high energy, frayed edge sites (FES)] and the basal plane of expandable layer silicates such as smectite and vermiculite (low-energy sites).

The clay-sized fraction of the Hanford sediment (smectite, chlorite, kaolinite, and mica) is small by mass (2–4% by wt), but accounts for a substantial portion of the low-affinity (basal plane) exchange sites that define the cation exchange capacity (CEC). This size fraction should be most susceptible to base attack because of its small grain-size. Equally, FES sites associated with micas edges may be altered by acid attack (Turpault and Trotignon, 1994; Kaviratna and Pinnavaia, 1995; Kalinowski and Schweda, 1996) and base attack (Samson et al., 2005), which arises because edge structures are more dissolution reactive than the basal plane. The large free hydroxide concentration of some leaked HLW fluids (~5 mol/L) could attack mineral edges and increase the rate of mica interlayer expansion, basal plane exposure, and K^+ release (Samson et al., 2005). These and other phenomena may affect the concentrations and site distributions of exchange sites, and their ion exchange selectivity for Cs^+.

Under alkaline pH conditions, aluminosilicate precipitates, and particularly zeolites, have been observed from dissolution

* Author to whom correspondence should be addressed (calvin.ainsworth@pnl.gov).

of kaolinite (Bauer et al., 1998), volcanic glass (Hawkins, 1981), Opalinus shale (Chermak, 1992, 1993), and fly ash (Lin and Hsi, 1995; Amrhein et al., 1996; Ma et al., 1998). In systems meant to simulate the high pH, saline, and aluminate concentrations of some Hanford HLW fluids cancrinite was observed to precipitate from suspensions of quartz (Bickmore et al., 2001), and chabazite and the zeolite-like feldpathoids sodalite and cancrinite precipitated from kaolinite suspensions that sorbed Cs^+ from the HLW fluids (Chorover et al., 2003). Exposure of Hanford sediment to simulated alkaline HLW fluid at elevated temperatures (60–200°C) resulted in the precipitation of cancrinite and analcime (an aluminosilicate zeolite), both of which sorbed/incorporated Cs^+ (Nyman et al., 2000). Similarly, cancrinite and sodalite precipitated from Hanford sediment when reacted with simulated alkaline HLW fluids at 50°C (Qafoku et al., 2003a, 2003b).

Sediment exposure to high pH solutions results in mineral dissolution, transformation, and secondary mineral precipitation. The impact of these reactions on Cs^+ sorption, however, is less certain. Here we investigate the effect of temperature, and base catalyzed dissolution on Cs^+ sorption behavior to a subsurface sediment typical of material beneath the HLW tanks at the Hanford site. The micaceous sediments used in these studies were those utilized by Zachara et al. (2002) to investigate the effect of electrolyte composition and concentration on Cs^+ adsorption. Sediments were reacted with 0.1 M NaOH at 10°C and 50°C for 168 days. At various stages, sediment samples were removed and washed with a $NaNO_3$ solution until supernatant pH was about 8, and then exposed to a range of Cs^+ concentrations (10^{-9}–10^{-2} mol/L) to investigate short-term (16 h) Cs^+ exchange. The impact of base dissolution on $Na \rightarrow Cs^+$ exchange was investigated through the calculation of conditional exchange constants and comparison to those determined by Zachara et al. (2002). A second set of studies followed the sorption of Cs^+ to the Hanford sediment in the presence of 0.1 M, 1 M, and 3 M NaOH over a 112-day period. Three Cs^+ concentrations were used in these studies to evaluate the evolving effects of base catalyzed dissolution on high, intermediate, and low Cs^+ adsorption densities. The aqueous chemical evolution of sediment exposed to 0.1 M, 1M and 3 M NaOH was followed with time. Electron microscopy, electron micoprobe, and XRD were used to delineate mineralogic changes to the sediment and a two site ion exchange model incorporating enthalpy effects was used to evaluate the effects of base contact on Cs^+ adsorption.

2. EXPERIMENTAL PROCEDURES

2.1. Sediment Preparation and Properties

A homogenized, composite sediment was prepared from core samples taken in the construction of four Resource Conservation Recovery Act (RCRA) monitoring wells surrounding the S-SX tank farm at the U.S. Department of Energy's Hanford site in Washington state. As previously described (Zachara et al., 2002), carbonate materials were removed by treatment with sodium acetate (NaOAc at pH 5) and the sediment exchange complex was Na-saturated. After this treatment, the cation exchange capacity (CEC) of the Na-saturated sediment was determined to be $4.26 \times 10^{-5} \pm 0.12 \times 10^{-5}$ eq/g (Zachara et al., 2002). The low CEC values reflect the small clay mass (<2%) of the sediment. Particle size distribution of the sediment categorized it as sandy silt. Sediment mineralogical analyses of the various particle sizes were performed by X-ray diffraction (XRD) and optical microscopy. For fractions >2 μm, quartz was dominant with lesser amounts of plagioclase, potassium feldspars, and micas. The micas were characterized as muscovite, biotite and vermiculitized biotite. The clay size fraction (<2 μm) consisted of smectite, chlorite (clinochlore), and mica (for a more detailed description of mineralogy see Zachara et al., 2002; Serne et al., 2002b).

2.2. Base Treatment of Sediments

Batch reactors were used to investigate the impact of NaOH on the Hanford sediment mineral assemblage and the sediment's affinity for $^{137}Cs^+$. Hydroxyl concentrations were set at about 0.1, 1.0, and 3.0 M. At 0.1 M NaOH, studies were performed at 10°C and 50°C with 1 M $NaNO_3$ as a background electrolyte. All other base concentration studies were conducted at 50°C with 1 M $NaNO_3$ electrolyte. Subsurface temperatures beneath the S-SX tank farm at Hanford have remained above 50°C for over 20 years due to the thermal load of radioactive decay in the stored HLW. A large solution to solid ratio (40) was used to minimize hydroxyl consumption resulting from sediment dissolution and secondary mineral precipitation. Aqueous solutions were analyzed for Al, Si, Ca, Mg, Fe, and K by ICP-MS (Perkin-Elmer Elan 5000) or ICP-AES (Perkin-Elmer 5000) depending on the dilutions required because of the high salt concentrations. Analytical standards and blanks were produced with the same materials used in preparing the sediment suspension solutions. The analysis of K^+ in these high sodium systems was difficult due to the need for large dilutions, potassium's fairly high detection limit with ICP-AES, and the potential for polyion interferences (e.g., Na-O) with ICP-MS. These analytical problems probably affected the absolute concentrations of K^+ but not the trends observed.

2.2.1. Sediment treated with 0.113 M NaOH

NaOAc-treated Hanford sediment was contacted with 0.113 M NaOH/1 M $NaNO_3$ for 1 hr, 4 hr, 8 hr, 1 d, 3 d, 7 d, 14 d, 28 d, 42 d, 56 d, 112 d and 168 d (for convenience, 0.113 M NaOH is hereafter referred to as 0.1 M). NaOH solutions and sediment suspensions were synthesized and kept under a $N_{2(g)}$ atmosphere throughout the studies to limit $CO_{2(g)}$ and $O_{2(g)}$ absorption. Suspensions were continuously agitated on an orbital shaker (30 rpm) for the first 3 days, and then vigorously agitated by hand for several minutes twice a day for the remaining days. The 56 d, 112 d, and 168 d samples used 250-mL Teflon bottles and carried six replicates; all other time period samples used Teflon Oak Ridge centrifuge tubes, and carried duplicate samples. Replication number was based on the need for ample sediment to perform specific analyses after each time period (i.e., CEC, Cs adsorption, and where feasible, XRD and SEM.). Identical sample sets were carried out at 50°C and 10°C.

The samples were centrifuged (5,000 RCF [relative centrifuge force] for 30 min) at temperature, placed in a $N_{2(g)}$ glove box, and the supernatant decanted for determination of pH, and Al, Si, Fe, Ca, Mg, and K for each sampling point. Most of the supernatant was immediately diluted (1 to 10 v/v) to prevent precipitation as the samples equilibrated to room temperature. A 3 to 5 mL sample of the original supernatant was utilized for pH determination, prior to any significant cooling (or warming) of the sample. After decanting the supernatant, the solids from replicate temperature and time elements were placed in a filter system (0.2 μm filter), and washed with a pH neutral solution of 0.1 M $NaNO_3$ wash five or six times (total volume ~ 40 mL), followed by pH 5.5 0.01 M $NaNO_3$ until the filtrate pH was at or below 8.0 (total volume ~ 10 mL). This was followed by a final wash with 0.01 M $NaNO_3$. All sample manipulation was performed under a $N_{2(g)}$ atmosphere. Sediments were air-dried and stored under a $N_{2(g)}$ atmosphere at room temperature.

2.2.2. Sediment treated with 1 M and 3 M NaOH

NaOAc-treated, Na-saturated Hanford sediment was contacted with 1M NaOH/1 M $NaNO_3$, or 3M NaOH/1 M $NaNO_3$ solutions at 50°C for 1 hr, 8 hr, 1 d, 7 d, 14 d, 28 d, 56 d, and 112 d. The sediments were treated and sampled as previously described. Only Al, Si, and K concentrations were determined for each sampling point because of the

large dilutions required. The pH was not determined for these materials. Sediments were air-dried and stored under a $N_{2(g)}$ atmosphere.

2.2.3. Cs exchange isotherms on 0.1 M NaOH pre-treated sediment

Cesium exchange isotherms were measured on washed, and pH adjusted (~8.0), base treated sediments (56 d, 112 d, and 168 d) in 1 M $NaNO_3$ electrolyte (see section 2.2.1). Post-treatment, air-dried sediments were washed three times in 1 M $NaNO_3$ and resuspended prior to addition of $CsNO_3$; the solids concentration was 50 g/L. Exchange measurements were performed in triplicate at 10^{-1}, 10^{-3}, 10^{-6}, and 10^{-9} M $CsNO_3$, and in duplicate at 10^{-2}, 10^{-4}, 10^{-5}, and 10^{-7} M $CsNO_3$. Radiolabeled ^{137}Cs (as CsCl in 0.1 M HCl with a specific activity of 3.7×10^6 mCi/mol) was added to yield 7000 to 20,000 dpm/mL ^{137}Cs. The suspensions were shaken for 16 h at room temperature (~20°C) in 50-mL polycarbonate tubes at 80 rpm. After equilibration, the aqueous phase was separated from the sediment by centrifugation at 5000 rcf for 30 min. The ^{137}Cs in the aqueous phase was determined by gamma radiation counting using a Wallac gamma counter, model 1480. The count window was set at 560 to 710 keV, yielding a counting efficiency of 0.207. Counting samples were determined by mass and counted for 24 h or until about 10,000 total counts were obtained. The exchange procedure in the current study followed precisely the procedure used by Zachara et al. (2002).

2.2.4. Time-dependent Cs sorption during NaOH attack

Time-dependent ^{137}Cs sorption at 10°C and 50°C was investigated in 0.1 M NaOH/1 M $NaNO_3$ at three Cs concentrations: 2.1×10^{-9}, 1.3×10^{-7}, and 4.5×10^{-5} M $CsNO_3$. Teflon Oak ridge centrifuge tubes (35-mL) were used as batch reactors. The three Cs^+ concentrations were selected based on results of Zachara et al. (2002), and were selected to populate various exchange site classes: 1) high affinity (4.26×10^{-11} mol/g), 2) transition (6.75×10^{-9} mol/g), and 3) low affinity (4.26×10^{-7} mol/g). Aqueous ^{137}Cs concentrations were determined in the centrifugates by gamma-radiation counting. At 50°C, ^{137}Cs was determined after 1 hr, 4 hr, 8 hr, 1 d, 3 d, 7 d, 14 d, 28 d, 42 d, 56 d, and 112 d of base contact in replicate samples. At 10°C, ^{137}Cs was determined after 14 d, 28 d, 56 d, and 112 d of base contact in replicate samples.

Similar time-variant sorption studies were conducted in 1 M NaOH/1 M $NaNO_3$and 3 M NaOH/1 M $NaNO_3$ at 50°C. These high base experiments used slightly higher concentrations of $CsNO_3$: 6.1×10^{-9}, 4.0×10^{-7}, and 1.3×10^{-4} M $CsNO_3$ in 1 M NaOH, and 1.3×10^{-8}, 8.8×10^{-7}, and 3.0×10^{-4} M $CsNO_3$ in 3 M NaOH. The different $CsNO_3$ concentrations were used to offset the expected decrease in Cs^+ sorption due to higher Na^+ concentrations. Duplicate samples were sacrificed to determine aqueous ^{137}Cs concentrations (by gamma-radiation counting) at 1 h, 8 h, 1 d, 7 d, 14 d, 28 d, 56 d, and 112 d.

2.3. pH/p[H] Determinations

The pH of the 1 M $NaNO_3$/0.1 M NaOH-sediment suspensions with time was determined using a combination pH glass electrode (Orion-Ross, semi-micro). Immediately after decanting the centrifugate a 3 to 5-mL sample was placed in a glove box under $N_{2(g)}$ atmosphere, at which time the pH was determined (see section 2.2.1). For this study, the ability to discern significant changes in pH as a function of time was more important than determining the precise pH value of the sediment suspension. However, because of concern of the possible salt effects (liquid junction potentials) and the high base concentration on pH measurements using a combination glass electrode, a series of Gran titrations of the 1 M $NaNO_3$ solution was performed (Rai et al., 1995). Solutions of 1 M $NaNO_3$ (25-mL aliquots) were titrated with standardized 0.1 M NaOH, or 0.1 M HNO_3 using a modified Gran titration in which the moles of added free acid (or base) were plotted against H^+_{obs} (pH). This technique has been generally used as a simple method for estimating the hydrogen ion concentration (p[H]) in concentrated salt solutions (1 to 6 M). The logarithm of the slope of the titration curve delineates the correction factor A in the relationship, $p[H] = pH_{ob} + A$ (Rai et al., 1995). In the current study this technique was utilized to determine the behavior of the electrode in 1 M $NaNO_3$ and 0.1 M NaOH, and the stability of the pH measurement.

2.4. XRD and SEM Analysis of Treated Sediment

The NaOH treated sediments at 50°C were separated into two particle sizes for X-ray diffraction (XRD) analyses. The sediments were dry-sieved at 53 μm to decrease the likelihood of mineral dissolution during separation. The <53 μm sediment fraction was analyzed as a semi-random powder-mount. Clay fractions (<2 μm) were obtained from the <53 μm isolate by centrifugation (Jackson, 1969). However, small quantities of the clay-sized fraction limited the XRD analyses to sediments treated with: 1) 0.1 M NaOH at 56 and 112 days, 2) 1 M NaOH for 7, 24, and 33 days, and 3) 3 M NaOH at 7, 24, and 33 days. The particle size separates were dried as soon as possible after separation. The <2 μm isolates were analyzed as oriented smear mounts.

The samples were analyzed using a Philips X'Pert MPD system employing the PW3050/10 vertical theta-theta goniometer and a PW3373 ceramic X-ray tube with Cu anode. Standard operating power was 2000 W (40 kV, 50 mA). Samples were examined from 2 to 80 degrees 2Θ. Powder samples were mounted in 12-mm diameter shallow cavities in off-axis single-crystal quartz plates (Gem Dugout, State College, PA.). Mineral identification utilized JADE+, V2.1 (Materials Data Inc., Livermore, CA.). The search-match algorithm used the JCPDS Powder Diffraction File reference database (International Centre for Diffraction Data, Newtown Square, PA.).

Scanning electron photomicrographs were collected using a JEOL 6340F scanning electron microscope (SEM), operated at an accelerating potential of 10 KeV and a beam current of 10 nA. The granular samples were mounted on conductive tape on aluminum stubs, and sputter coated with carbon to assure electrical conductivity. Qualitative compositional data were collected during imaging using an Oxford Isis energy-dispersive spectrometer (EDS).

2.5. CEC Determinations

The CEC of the 0.1 M NaOH-treated sediment (section 2.2.1) was determined at 56 d, 112 d, and 168 d as previously described (Zachara et al., 2002). Briefly, after being air-dried, a prescribed mass of sediment was placed in Oak Ridge centrifuge tubes and washed three times with 0.002 M $NaNO_3$ solution to obtain a low $[Na]_{aq}$ in the occluded solution prior to addition of the radiotracer solution. Isotopic exchange with ^{22}Na in 0.002 mol/L $NaNO_3$ electrolyte was used to determine the Na-based CEC (Babcock and Schultz, 1970). The aqueous phase activity of ^{22}Na after 16 h equilibration was determined using a Packard 2550 TR/LL liquid scintillation analyzer and Hionic-Fluor (Perkin-Elmer). As with ^{137}Cs, counting samples were determined by mass and counted for 24 h or until about 10,000 total counts were obtained.

3. RESULTS AND DISCUSSION

In this section, we first address the effect of base on the aqueous phase, and solid phase composition. Of particular importance are i) the relationship between base concentration and onset of precipitation; ii) solid precipitate identification; and iii) changes in CEC, which could have significant affects on Cs^+ sorption. Next, we show and discuss results relevant to the effect of base on Cs^+ sorption to i) Hanford sediment that had been reacted with 0.1 M base, washed, pH adjusted back to near-natural pH (~8.0), and then reacted with Cs^+; and ii) the effect of 0.1 M, 1 M, and 3 M base with time on Cs^+ sorption when sediment, base, and Cs^+ are present from t = 0. Finally, the Cs^+ adsorption data are compared to pristine sediment Cs^+ sorption data through the use of a two-site ion exchange model (Zachara et al., 2002), and variations between base-reacted and pristine sediment focuses on solid phase changes discussed previously.

3.1. Evolution of Aqueous Phase Composition in the Presence of Base

In order to estimate the changes in pH in the high salt, high base systems of the current study the technique of Rai et al. (1995) was used to estimate the salt effect on the hydrogen ion concentration (p[H] = $pH_{obs.}$ + A). Titration of 1 M $NaNO_3$ with standardized NaOH yielded a series of linear relationships that were essentially identical, and a correction factor (A) equal to 0.79. The linearity of the titration data, and its reproducibility suggested that pH measurements in the present system would be stable and that significant change in pH with time could be easily detected. The p[H] of the sediment suspension in 0.1 M NaOH and 1 M $NaNO_3$ was fairly constant over the entire length of the study. The initial p[H] determinations (at about 2 h) were 13.3 and 13.4 (pH 12.5 and 12.6) at 50°C and 10°C, respectively. Neither the p[H] or pH exhibited any observable pattern indicative of substantial OH consumption with time; the maximum p[H] or pH variation over the study period was about 0.2 units.

The release of Al and Si showed contrasting trends in the variable concentration NaOH systems at 50°C (Fig. 1a, b). Aluminum rapidly dissolved to a maximum, then sharply decreased with equilibration time. Si_{aq} began to plateau before Al_{aq} reached its maximum, and then increased slightly (1 M and 3 M NaOH) toward the end of the study. The time required to attain the maximum Al_{aq} was approximately 42, 28, and 14 days at 0.1 M, 1 M, and 3 M NaOH, respectively. During the initial dissolution phase (≤7 days depending on base) the Si_{aq}/Al_{aq} molar ratio was virtually the same (3.7 to 5; Fig 1c). Beyond this initial period, the Si_{aq}/Al_{aq} ratio began to increase, and the extent of increase was dependent on base concentration. The dramatic drop in Al_{aq} and the increase in Si_{aq}/Al_{aq} ratio signified the precipitation of secondary minerals. The precipitation reactions, however, undoubtedly began before the Al_{aq} maximum was attained.

In contrast to the 50°C data, the 10°C evolution profiles of Al_{aq} and Si_{aq} increased to poorly defined maxima between 84 and 112 days (Fig. 2a, b). The Al_{aq} and Si_{aq} maxima were approximately one-half and one-third, respectively, of that observed at 50°C. The Si_{aq}/Al_{aq} exhibited a near constant value (10.1–12.4) over 112 days (Fig. 2c). Between 112 and 168 days, Al_{aq} and Si_{aq} exhibited a slight decrease in concentration, and the Si_{aq}/Al_{aq} deceased by about a factor of 2. While the decrease in Al_{aq} and Si_{aq} (at both temperatures) signaled precipitation of secondary minerals, the difference in Si_{aq}/Al_{aq} evolution with temperature was completely opposite.

Bauer and Berger (1998), investigated kaolinite dissolution in the presence of KOH using a batch reactor. They observed an initial pure dissolution phase whose instantaneous Si solubilization rate was inversely dependent on Al_{aq}. The dissolution phase was followed by a second stage that corresponded to a precipitation phase, whose onset disrupted the Si solubilization rate dependence on Al_{aq} and was dependent on temperature and $[OH^-]$ (Bauer and Berger, 1998; Bauer et al., 1998). In the current study, assuming $[Al_{tot}]_{aq} \approx [Al(OH)_4^-]$, the instantaneous rate of Si solubilization exhibited an early inverse dependence on the $[Al(OH)_4^-]/[OH^-]$ (Fig 3a, b). However, as $[Al(OH)_4^-]/[OH^-]$ increased the rate of Si solubilization became almost constant. The constancy in Si release rate is

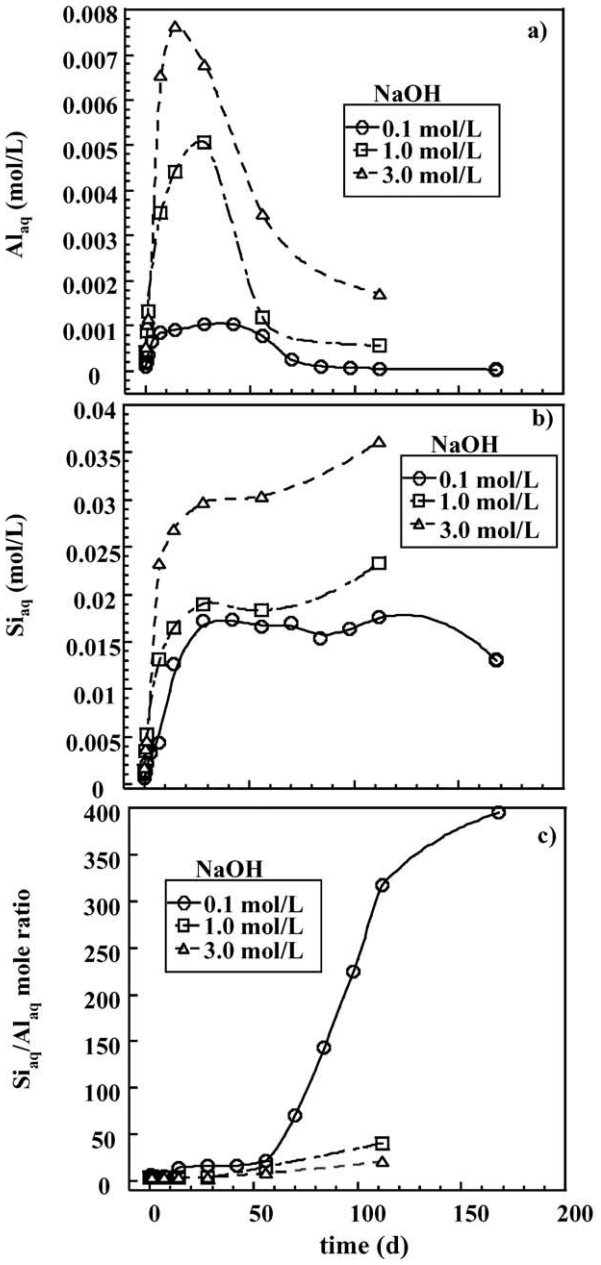

Fig. 1. Aqueous concentration of a) Al, b) Si, and c) Si/Al ratio as a function of time for Hanford sediment in contact with 0.1 M, 1 M, and 3 M NaOH in 1 M $NaNO_3$ at 50°C.

believed to reflect the onset of precipitation. At 10°C, this occurs at about $[Al(OH)_4^-]/[OH^-] \approx 0.0055$ (Fig. 3a), and at approximately $[Al(OH)_4^-]/[OH^-] \approx 0.002$ at 50°C regardless of base concentration (Fig. 3b). These $[Al(OH)_4^-]/[OH^-]$ ratios were attained between 84 and 98 days at 10°C in 0.1 M NaOH, and at 7 days, 4 days and 2 days at 50°C in 0.1 M, 1 M, and 3 M NaOH, respectively.

3.2. Base Effects on Sediment Mineralogy

The sediment developed red coloration with increasing time of base contact, and the intensity of the coloration increased

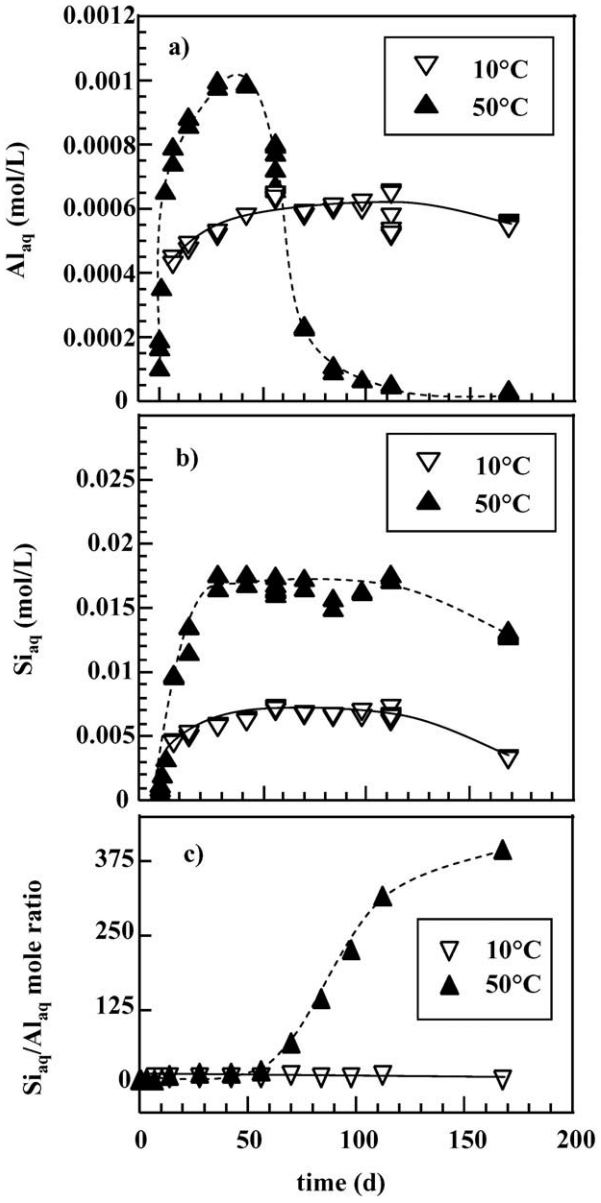

Fig. 2. Aqueous concentration of a) Al, b) Si, and c) Si/Al ratio as a function of time for the Hanford sediment in contact with 0.1 M NaOH and 1 M $NaNO_3$ at 10°C and 50°C.

with increasing base concentration at 50°C. By day 7, SEM micrographs and EDS analyses of sediment reacted with 1 M and 3M NaOH showed the presence of small, iron oxide clusters made up of individual spherical submicron Fe particles (micrographs not shown). Fe oxides of similar morphology were observed after 112 days at the lowest base concentration. Fe(III)oxide formation resulted from biotite and chlorite dissolution followed by oxidation of solubilized Fe(II). At 10°C, no visual changes to sediment color were evident, nor were there any significant mineralogic changes that could be discerned by XRD.

After exposure to 0.1 M NaOH for 56 d at 50°C, XRD patterns of Hanford sediment clay-sized fraction (<2 μm) showed a secondary precipitate coexisting with residual mica,

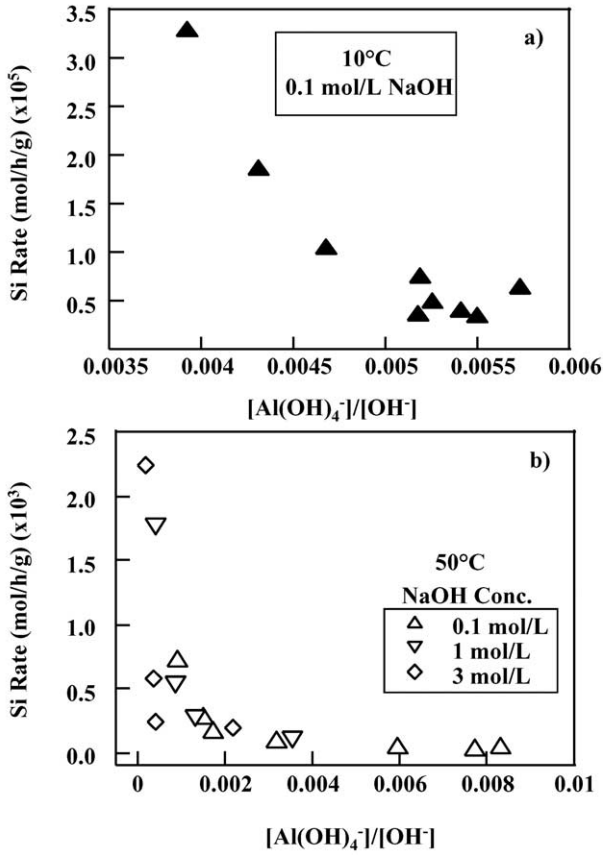

Fig. 3. Instantaneous Si dissolution rate as a function of the $Al(OH)_4^-/OH^-$ ratio at a) 10°C and b) 50°C (only rate data prior to Al attaining its maximum concentration are presented for 50°C).

chlorite, quartz, and smectite (T in Fig. 4). The secondary precipitate was identified as tetranatrolite, a zeolite ($Na_2Al_2Si_3O_{10}\cdot 2H_2O$), that has been known to occur in saline or salt affected soils at elevated pH (Ming and Mumpton, 1989). Comparison of diffraction maxima between the 56-d, 112-d and 168-d samples (data not shown) suggested increasing tetranatrolite, and decreasing phyllosilicates with base contact time. At the higher base treatments (1 M NaOH/1 M

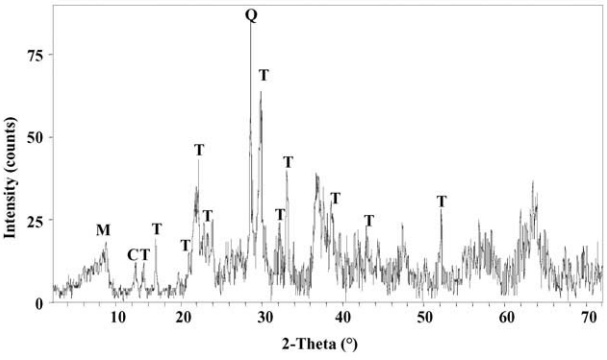

Fig. 4. X-ray diffraction pattern of the <2 μm fraction of Hanford sediment after 112 days in contact with 0.1 M NaOH in 1 M $NaNO_3$ at 50°C (Q = quartz, M = mica, C = chlorite, and T = tetranatrolite).

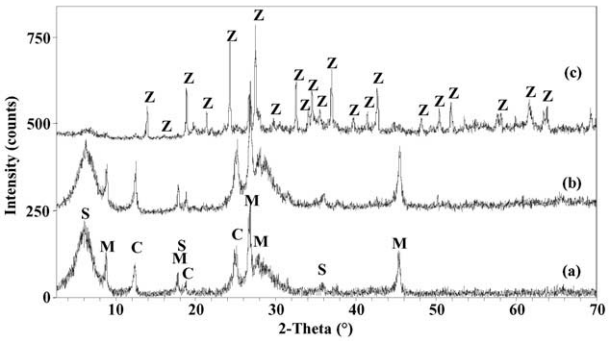

Fig. 5. X-ray diffraction pattern of the <2 μm fraction of Hanford sediment after a) 7 days, b) 24 days, and c) 33 days in contact with 1 M NaOH in 1 M $NaNO_3$ at 50°C (s = smectite, M = mica, C = chlorite, F = feldspar, and Z = unnamed $Na_2Al_2Si_3O_{10}{\cdot}2H_2O$ phase).

$NaNO_3$ and 3 M NaOH/1 M $NaNO_3$) the steady disappearance of phyllosilicate diagnostic diffraction peaks was more pronounced. By 33 days the <2 μm fraction smectite, mica, and chlorite diffraction maxima were barely observable, and new set of diffraction maxima (marked by Z) associated with an unnamed neoform ($Na_{14}Al_{12}Si_{13}O_{51}{\cdot}6H_2O$) were revealed (Fig. 5). The secondary phase ($Na_{14}Al_{12}Si_{13}O_{51}{\cdot}6H_2O$) was identified by the search-match algorithm as JCPDS #28-1036. A similar sodium aluminum silicate hydrate mineral phase had been observed to precipitate in fly ash treated with 3 M NaOH at 100°C (Amrhein et al., 1996).

SEM examination of the >53 μm fraction reacted with 0.1 M base showed clear evidence of secondary precipitation on quartz, feldspar, and biotite particles, and NaOH attack on mica (particularly biotite) (Fig. 6). Over the 168-day exposure to 0.1 M NaOH at 50°C, quartz particles exhibited little evidence of dissolution (Fig. 6a, b, c). With time, however, secondary precipitates accumulated on all mineral surfaces. EDS analysis of secondary precipitates on quartz surfaces had a Na-Al-Si-O composition with morphology illustrated by Figure 6d. Biotite samples isolated from pristine sediment exhibited surfaces clear of precipitates, with sharp, clean edges (Fig. 6e). After 168 days in 0.1 M NaOH, the biotite surfaces were crenulated, the edges were dulled, and curled, and secondary precipitates were clearly present (Fig. 6f).

SEM inspection of the >53 μm sediment fraction exposed to 1 M and 3 M NaOH showed the same basic trends observed for the 0.1 M NaOH treatment (Fig. 7). The accumulation of

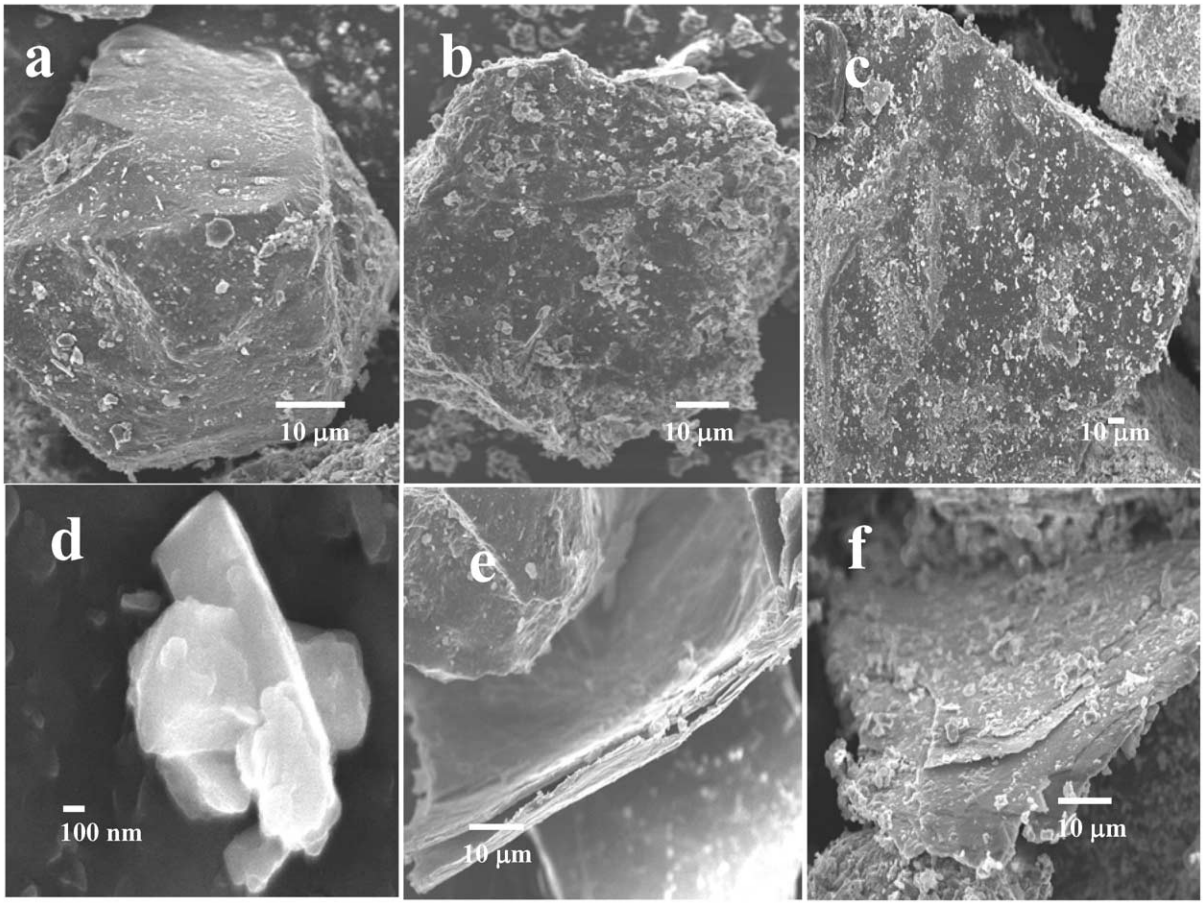

Fig. 6. Electron micrographs of mineral phases from the Hanford sediment (>53 μm fraction) after exposure to 0.1 M NaOH in 1 M $NaNO_3$ at 50°C for selected time periods: a) quartz particle, t = 56 d; b) quartz particle, t = 112 d; c) quartz particle, t = 168 d; d) suspected secondary tetranatrolite on quartz particle t = 168 d; e) pristine biotite; f) biotite t = 168 d.

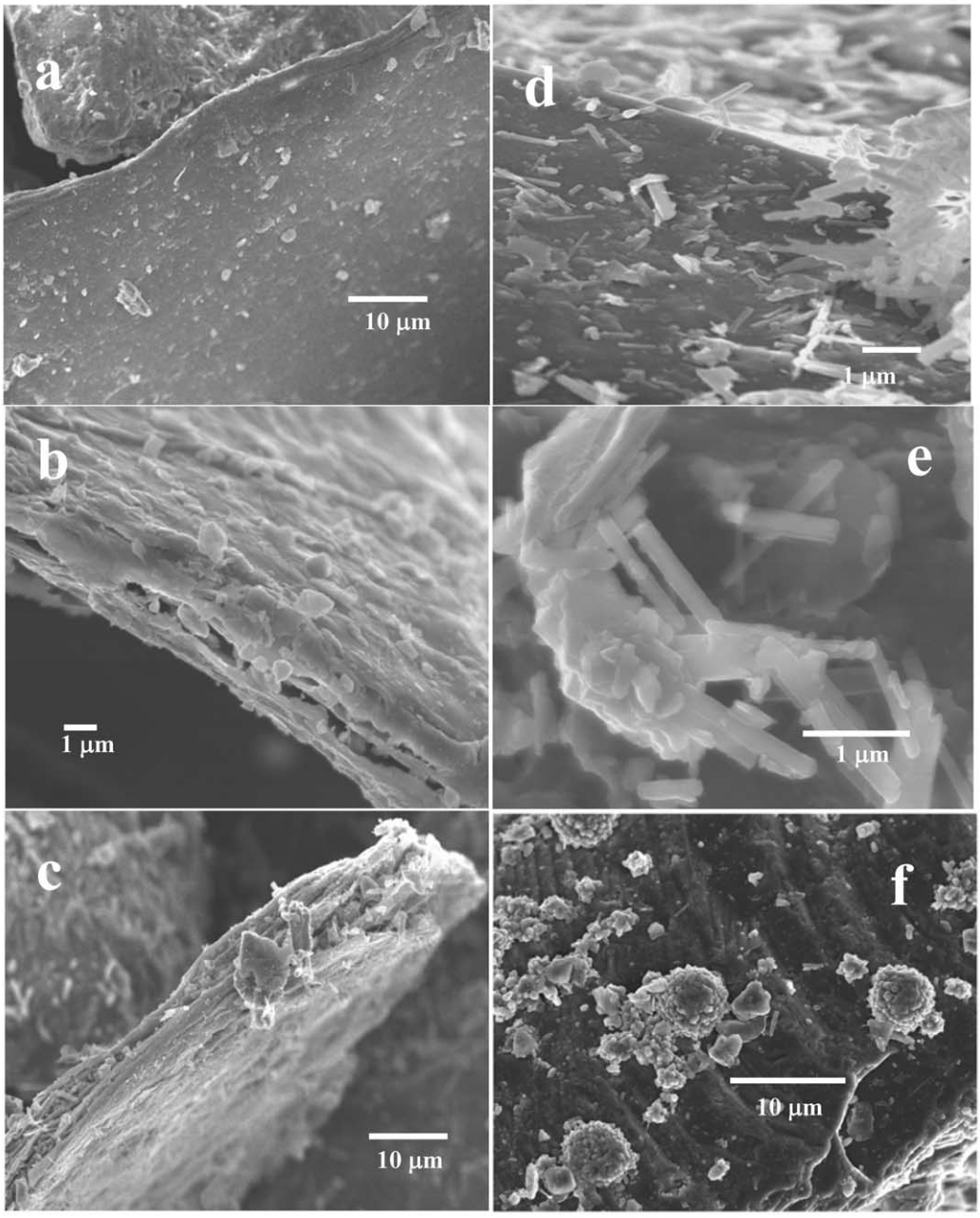

Fig. 7. Electron micrographs of mineral phases from the Hanford sediment (>53 μm fraction) after exposure to 1 M, or 3 M NaOH in 1 M $NaNO_3$ at 50°C for selected time periods: a) biotite, 1 M NaOH, t = 7 d; b) biotite, 1 M NaOH, t = 24 d; c) biotite, 3 M NaOH, t = 33 d; d) quartz grain with surface precipitate of $Na_2Al_2Si_3O_{10}{\cdot}2H_2O$, 1 M NaOH, t = 33 d; e) higher magnification of d; f) feldspar with secondary precipitate of $Na_2Al_2Si_3O_{10}{\cdot}2H_2O$, 3 M NaOH, t = 7. The precipitates in e, and f show clearly different morphologies, but exhibit identical Si/Al ratios and composition (as determined by EDS).

secondary precipitates on quartz, feldspar, and mica (particularly biotite) increased with base contact time, and as the NaOH concentration was increased. The biotite particles showed similar edge and surface deterioration after just 7 to 24 days of contact time with 3 M and 1 M NaOH as compared to 168 days at 0.1 M NaOH (compare Fig. 6e, f with Fig. 7a–c). As with the 0.1 M NaOH treated sediments, secondary precipitates in the 1 and 3 M NaOH treatments tended to accumulate on all mineral surfaces. The secondary precipitates observed at 1 M NaOH appeared as rod-like structures that with time, clustered together (Fig. 7d, e). With 3 M NaOH, the secondary precipitates exhibited hemisphere morphology (Fig. 7f). The precipitated $Na_{14}Al_{12}Si_{13}O_{51}{\cdot}6H_2O$ appears zeolite-like in both structures and the composition.

The precipitation of zeolite and zeolite-like minerals from highly basic mineral suspensions was not unexpected (see section 1.0). The absence of cancrinite formation was also not surprising with the absence of aluminate in the initial contact

Table 1. Cation exchange capacities of Hanford sediment as a function of time and temperature of exposure to 0.1 M OH.

Saturating ion	Base exposure (d)	CEC (eq/g × 10^{-5})[a] 10°C	50°C
Na	0	4.26 ± 0.12	
	56	2.25 ± 0.03	4.71 ± 0.13
	112	3.08 ± 0.16	6.73 ± 0.11
	168	3.06 ± 0.07	7.42 ± 0.84

[a] The initial CEC (time = 0) is taken from Zachara et al. (2002) where n = 6; the other time period CEC values were determined in this study with n = 3.

solution. Qafoku et al. (2003a, b) investigated the dissolution/precipitation of Hanford sediment in contact with solutions identical to the current study (1 M NaOH/1 M $NaNO_3$; at 50°C) except with increasing Al concentrations (0.055 mol/L to 0.22 mol/L). Even the lowest aluminate contact solutions were oversaturated with respect to cancrinite, and exhibited Si/Al molar ratios between 0.096 and 0.284, which is as much as 10 to 50 times less than the current study's Si/Al ratio (Fig. 1c). While the solution data from the current study were not modeled, a comparison of current Si/Al ratios to that of Qafoku et al. (2003a, b), Barnes et al. (1999) and Bickmore et al. (2001) suggests that the present system was always undersaturated with respect to the cancrinite. The precipitation of zeolites or zeolite-like secondary mineral phases from mineral dissolution in the current high pH, saline solutions, or Al-chabazite (Chorover et al., 2003) from kaolinite—high pH, saline solutions aluminate suspensions—arise because of temperature and initial solid phase differences. In the more complex aluminate suspensions aqueous-mediated transformation has been suggested to follow as aluminosilicate species → amorphous phase → zeolite → sodalite → cancrinite (Barnes et al., 1999).

3.3. Changes in Sediment CEC After Exposure to 0.1 M NaOH

At 10°C, the sediment exhibited a substantial decrease in CEC within 56 days (47%), followed by an increase after 168 days to approximately 72% of its original CEC. At 50°C and 0.1 M NaOH, the sediment showed a steady increase in CEC, which by the end of the experiment had increased by 74% to 7.42 ± 0.84 × 10^{-5} eq/g (Table 1). The increase at 50°C was well represented by a linear model (R = 0.976) whose slope equated to a growth in CEC of 2.04×10^{-7} eq/g/d. The increase in CEC observed at 50°C was expected (discussed below), but the trend in CEC at 10°C was not. The apparent decrease in CEC at 10°C may have resulted from incomplete K^+ removal during the post-base treatment washing process which would hinder an accurate determination of CEC. If the $NaNO_3$ washing of base treated sediment did not effectively remove the exchangeable K^+, the CEC measurements would probably be understated for both temperatures.

Using the same sediment as the current study and Zachara et al. (2002), Steefel et al. (2003) determined a CEC of 12.19 × 10^{-5} eq/g based on the equivalent sum of cations eluted by a pre-flush of a sediment column using 1 M $NaNO_3$ or 1 M KNO_3; similarly, ^{22}Na elution from a sediment column yielded a CEC of 12.0 × 10^{-5} eq/g. Using the ^{22}Na batch technique similar to that used by Zachara et al. (2002) and the current study, Steefel et al. (2003) found the CEC substantially lower and similar to that of Zachara et al. (2002); 4.6 × 10^{-5} eq/g. With pristine Hanford sediments, apparent Na-saturated material contained appreciable residual Ca^{2+} not exchanged by Na^+, and resupplied by feldspar dissolution while in suspension. This residual Ca^{2+} must be considered for accurate CEC determination. In the present study, residual K^+ could have had a similar effect at both temperatures. However, for the comparative purposes of this study's sediment Cs^+ exchange with that of Zachara et al. (2002), the use of the same CEC determination technique was required.

The increase in CEC observed in sediment exposed to 1 M NaOH/1 M $NaNO_3$ at 50°C probably resulted from interlayer expansion of micas (particularly the more reactive biotite). Interlayer expansion exposed interlayer K^+ to exchange, and increased the CEC. Potassium release from biotite between pH 2 to 10, showed an initial rapid release through ion exchange, followed by diffusion-controlled release of interlayer ions as the mica layers expanded (Malmström and Banwart, 1997). Under base attack Samson et al. (2005) observed essentially no dissolution of biotite basal surfaces, but grain edges were exfoliated and splayed. The dissolution of biotite has been correlated primarily with edge surface area (Turpault and Trotignon, 1994; Trotignon and Turpault, 1992 as reported by Nagy, 1995). In the current study, basal surfaces showed signs of weathering, but it was the mica edges that exhibit significant changes after reaction with base (Fig. 6 and 7).

Concomitant with base attack of micas, the formation of tetranatrolite could also contribute to the observed CEC increase at 50°C. As stated previously, tetranatrolite is part of the natrolite subgroup of zeolites. These zeolites are characterized as fibrous, small-pore zeolites whose framework is composed of T_5O_{10} units formed from linking five TO_4 tetrahedra (T = Al, Si) that are then connected along the c-axis to form natrolite chains (Lee et al., 2002). Charge balancing cations (e.g., Na, K etc) reside along the channels created by c-axis linkages. Tetranatrolite and natrolite differ in disorder degree in the tetrahedral sites; the latter exhibiting almost complete disordering (Lee et al., 2000). The small pores associated with natrolite limits cation exchange between Na^+ and large radius monovalent cations such as Cs^+, and divalent cations (e.g., Sr^{2+}). In studies with a natural natrolite at 60°C, Ca, Sr, Cs, Rb, and Mn, exchange for Na was less than 2% of the total available exchange sites while K exchange accounted for 42% of the available sites (Dyer and Faghihian, 1998). Even with the restricted pore size, tetranatrolite's exchangeable Na^+ could contribute to CEC measured by ^{22}Na exchange.

3.4. Cs^+ Exchange/Selectivity with 0.1 M NaOH Treated Hanford Sediment at pH 8

Na-saturated Hanford sediment was exposed to 0.1 M NaOH/1 M $NaNO_3$ solution at 10°C or 50°C for 56, 112 or 168 days, washed free of base, pH adjusted to pH 8, and air-dried. Short-term (16 h) Cs^+ adsorption studies (total Cs^+ concentrations 10^{-9} to 10^{-1} mol/L) with washed sediment in 1 M $NaNO_3$ yielded Cs^+ adsorption isotherms that were of the Freundlich type with slopes (1/n) <1, suggesting sorption site

heterogeneity. A comparison of this study's isotherm data with those from Zachara et al. (2002), at the same solid to solution ratio (50 g/L) and 1 M $NaNO_3$, showed no substantive differences between the data regardless of sediment pretreatment (data not shown).

In order to isolate possible effects of base exposure on Cs^+ adsorption, conditional ion-exchange equilibrium constants (K_c) were computed from the short-term Cs^+ adsorption isotherm data. Calculated K_c's were based on the $Na^+ \rightarrow Cs^+$ exchange reaction

$$Cs^+_{(aq)} + NaX = CsX + Na^+_{(aq)}, \quad \text{with} \tag{1}$$

$$K_c = [Na^+][E_{CsX}]/[Cs^+][E_{NaX}], \tag{2}$$

where [] denotes concentration. E_{CsX} and E_{NaX} are the surface equivalent fractions for Cs^+ and Na^+ calculated as

$$E_{CsX} = q_{Cs}/Q \tag{3}$$

where q_{Cs} = the adsorption density in eq/g, Q = the appropriate time dependent CEC (eq/g), and $E_{NaX} = 1 - E_{CsX}$.

For sediments pretreated with 0.1 M NaOH/1 M $NaNO_3$ at 10°C, the $Na^+ \rightarrow Cs^+$ exchange ${}^{Cs}_{Na}K_c$ showed no clear evidence of time dependence over the range of E_{CsX} investigated (Fig. 8a). While there was some fluctuation in ${}^{Cs}_{Na}K_c$ with time (the 112-d values are slightly lower, and the 168-d values are slightly higher than the 56-d values), there was no consistent trend of changing ${}^{Cs}_{Na}K_c$ with base exposure. The fact that there was no clear base contact-time dependence indicated that the exchanger phase selectivity was not altered over the time period of the study. In contrast, the ${}^{Cs}_{Na}K_c$ values for the 50°C pretreated sediment showed a small but consistent trend of decreasing selectivity with increasing base contact time (Fig. 8b). The $\Delta^{Cs}_{Na}K_c$ for Cs^+ sorption densities below log E_{CsX} = −2.5 were approximately 0.2 to 0.4 log units after 168 days. The displacement at the higher log E_{CsX} values (>−2) was more difficult to discern due to data variability. While not significant, there was a perceptible displacement toward lower Cs^+ adsorption densities with base pretreatment exposure time.

The short-term Cs^+ adsorption data were modeled using the multi-site ion exchange model (Zachara et al., 2002), and the CEC measured at t = 112 days (Table 1). These fitted data were compared to a calculated log ${}^{Cs}_{Na}K_c$ versus log E_{CsX} curve based on the constants and concentrations for the two exchange sites [K_c(I) = FES sites; K_c(II) = planar sites] developed for pristine Hanford sediment by Zachara et al. (2002). Modeling results are shown in Table 2, and Figure 8a, b.

For the 10°C base pretreated sediments, the two-site ion exchange model described the Cs^+ sorption data well (Fig. 8a; solid line). The fitted log ${}^{Cs}_{Na}K_c$ versus log E_{CsX} curve was essentially identical to that calculated for pristine Hanford sediment except the fitted curve was uniformly displaced upward over the entire range of E_{CsX} by about log ${}^{Cs}_{Na}K_c$ = 0.45 (compare K_c(I) and K_c(II) values). The log ${}^{Cs}_{Na}K_c$ displacement, however, disappeared when E_{CsX} and ${}^{Cs}_{Na}K_c$ values were calculated based on the pristine sediment's CEC (data not shown). This result suggests that there was an underestimation of CEC for the 10°C pretreated sediment, probably as a result of incomplete saturation of the sediment prior to the short-term Cs^+ sorption study. Also, exposure to 0.1 M NaOH/1 $MNaNO_3$ at 10°C had little effect on Hanford sediment Cs^+ selectivity.

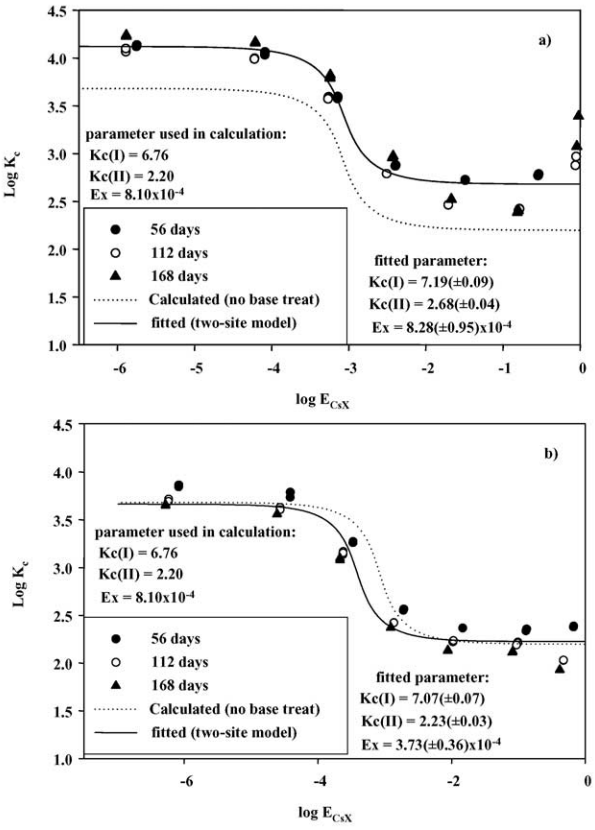

Fig. 8. Conditional equilibrium constants (${}^{Cs}_{Na}K_c$) for Cs^+ in Na^+ electrolyte at pH 8.0 after pretreatment with 0.1 M base for 56, 112, and 168 days at a) 10°C, and b) 50°C; the two-site cation exchange model results for (dashed line) the K_c prediction for Cs sorption to pristine Hanford sediment (from Zachara et al., 2002), and (solid line) the fitted K_c for the base treated sediment; Ex values are the FES site concentrations listed in Table 2.

The two-site ion exchange model (based on t = 112 d CEC) described Cs^+ sorption to the 50°C base pretreated sediment well (Fig. 8b). In comparison to the calculated selectivity for pristine sediment, the base treated sediment's K_c(I) was slightly higher 6.76 and 7.19, respectively), but the K_c(II) values were identical. The effect of base pretreatment was reflected, however, in the modeling by the decreased fraction of high-energy sites (Ex in Fig. 8b), which translated to a decrease from 3.45 × 10^{-8} eq/g in pristine materials to 2.94 × 10^{-8} eq/g base pretreated sediment; a 15 % loss of FES sites over a 112 day period.

Short-term Cs^+ sorption to base pretreated sediment and the model simulations of the sorption data correlated well with the mineralogic examination of reacted sediment. At 10°C, no significant mineralogic changes were observed, and Cs^+ sorption and model simulations were essentially identical to that of the pristine sediment. At 50°C, the post reacted sediment showed limited loss of clay-sized phyllosilicates, base attack to the edges of mica, and the precipitation of tetranatrolite. These base induced mineralogic changes were reflected in the short-term Cs^+ sorption and subsequent model results by a slightly

Table 2. Multiple site modeling parameters for Cs^+ sorption by pristine Hanford sediment, and sediment after 112 days exposure to 0.1 M NaOH at 10°C and 50°C.

Citation	Site type[a]	Site concentration X[b]	Site concentration Ex[c]	Selectivity coefficient (log K_c)
Zachara et al (2002a)		$CEC_{Na} = 4.26\times10^{-5}$ eq/g		
Measured at 30°C	FES	3.45×10^{-8} eq/g	8.1×10^{-4}	Na-Cs = 6.76 ± 0.6
	Planar	4.26×10^{-5} eq/g	0.999	Na-Cs = 2.20 ± 0.1
		$CEC_K = 8.25\times10^{-5}$ eq/g		
	FES	2.72×10^{-8} eq/g	3.3×10^{-4}	K-Cs = 4.73 ± 0.10
	Planar	8.25×10^{-5} eq/g	0.999	K-Cs = 0.96 ± 0.057
This study (Fig. 11)		10°C; 112 d $CEC_{Na} = 3.08\times10^{-5}$ eq/g		
Measured at 25°C	FES	2.55×10^{-8} eq/g	8.28×10^{-4}	Na-Cs = 7.19 ± 0.6
	Planar	3.08×10^{-5} eq/g	0.999	Na-Cs = 2.68 ± 0.1
		50°C; 112 d $CEC_{Na} = 6.73\times10^{-5}$ eq/g		
	FES	2.51×10^{-8} eq/g	3.73×10^{-4}	Na-Cs = 7.07 ± 0.6
	Planar	6.73×10^{-5} eq/g	0.999	Na-Cs = 2.23 ± 0.1

[a] Site type refers to frayed edge sites (FES) and the basal plane sites (Planar) that represent the cation exchange complex in the multiple site model.
[b] Total concentration.
[c] E_x = site concentration/CEC_n; where n denotes saturating cation or temperature.

higher K_c(I) value, higher CEC, and a small calculated decrease in FES site population compared to a pristine sediment. At both temperatures, however, Cs^+ adsorption densities were almost identical to those observed by Zachara et al. (2002) for pristine sediment.

3.5. Cs^+ Behavior with Hanford Sediment During Base Attack at 0.1 M NaOH

In pristine Hanford sediment, Cs^+ sorption kinetics (at 25°C) varied with electrolyte (Na) concentration and $[Cs^+]_{total}$. A steady-state Cs^+ adsorption density was attained within 12 h and maintained for 120 d in 5 mol/L $NaNO_3$ and 10^{-4} mol /L $CsNO_3$, but at 0.005 mol/L $NaNO_3$ Cs^+ adsorption reached its maximum in 12 h and then declined by 21% over 120 d (Zachara et al., 2002). At 0.1 mol/L $NaNO_3$ and 3.2×10^{-7} mol/L $CsNO_3$, 90% of the eventual steady-state adsorption density was attained within 12 to 24 h, and steady-state conditions were attained in 10 d (Liu et al., 2003b). In contrast to pristine sediments, Cs^+ adsorption to Hanford sediment in contact with 0.1 M NaOH/1.0 M $NaNO_3$ increased throughout the 112-d study regardless of $[Cs^+]_{total}$ or temperature (10°C or 50°C) (Fig. 9a, b, c). Only at 50°C and the highest targeted adsorption density did Cs^+ adsorption reach a temporary (~7 d) stable surface density (Fig 9c). Cs^+ adsorption at 10°C was not followed prior to 14 d.

Adsorption of Cs^+ was greater at 10°C at the low and intermediate surface densities (Fig. 9a, b), which was in line with the negative Na–Cs ion exchange enthalpies for high-energy (−17.87 ± 2.01 kJ/mol) and low-energy (−4.82 ± 0.44 kJ/mol) sites associated with pristine Hanford sediment (Liu et al., 2003a). These negative enthalpies translated into a Δ log Kc(I) and K(II) of −0.20 and −0.74 for Cs^+ exchange as the temperature increased from 30°C to 65°C (Liu et al., 2003a). At the highest surface density (Fig. 9c) Cs^+ sorption was contrary to the results of Liu et al. (2003a) (discussed below).

As a comparison, Cs^+ sorption to the Hanford sediment during base attack (depicted in Fig. 9) was simulated using the two-site ion exchange model of Zachara et al. (2002). Model simulations were based on CEC, K_c(I) and K_c(II), and site populations determined from short-term Cs^+ exchange studies conducted after the sediment was reacted with base for 112 d (Section 3.5; Table 2). The high- and low-energy site K_c values were corrected for temperature based on the enthalpy values from Liu et al. (2003a) (Table 3). The results of these calculations are depicted in Figure 9 by a dashed line (10°C), or a solid line (50°C).

The slow increase in Cs^+ sorption observed at 10°C from 14 d to 112 d is reminiscent of a slow steady increase in exchange sites; however, this is difficult to reconcile with the CEC measurements (section 3.4), and the minimal effect base attack had on ${}^{Cs}_{Na}K_c$ (section 3.5). Yet, the model simulations match the 112-d Cs^+ sorption data well at all three surface densities (Fig. 9). Given these results, coupled with no detectable changes in mineralogy (section 3.3), and the lack of variation in ${}^{Cs}_{Na}K_c$ after exposure to 0.1 M NaOH for up to 168 days it appears that sediment dissolution at 10°C and 0.1 M NaOH had no observable effect on Cs^+ sorption to Hanford sediment.

The 50°C, 112-d Cs^+ adsorption densities were consistently under-predicted by the model simulations (Fig. 9a, b, c). While the lower targeted Cs^+ adsorption densities were only slightly under-predicted (16%), the highest Cs^+ surface density was under-predicted by 57%. A 0.65 log unit increase in the Kc(I) was required to match the highest Cs^+ sorption experimental data. These results suggested that Cs^+ sorption to the Hanford sediment during base attack (0.1 M NaOH/1 M $NaNO_3$) at 50°C altered the site selectivity, or generated sorption sites that were not captured in the short-term Cs^+ sorption studies [from which the Kc(I and II) were generated; section 3.5, Fig. 8], and were not altered/formed at 10°C.

Cs^+ sorption (50°C) at the highest Cs^+ adsorption density was static for 7 days, and then increased through the rest of the study (Fig. 9c); the increased sorption correlated to the onset of tetranatrolite precipitation. These data suggested that increased Cs^+ sorption at 50°C was related to tetranatrolite precipitation, probably via ion exchange or inclusion within the precipitate. While the small pores associated with natrolite-type zeolites limit cation exchange between Na^+ and large radius monovalent

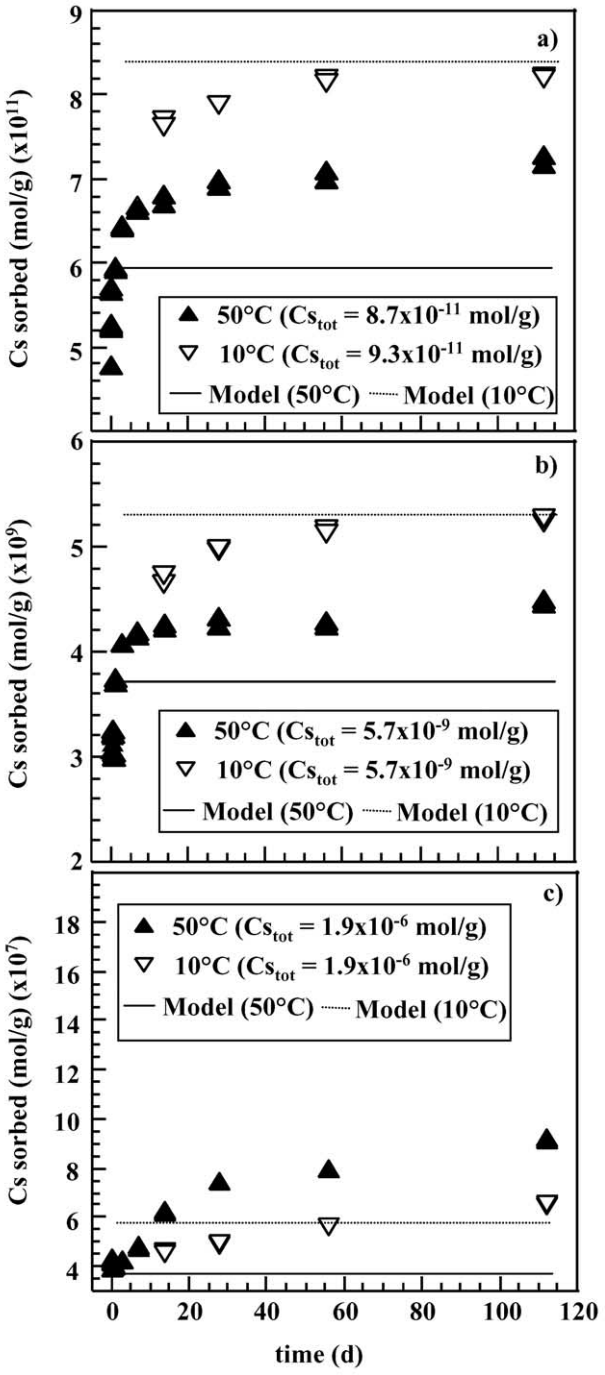

Fig. 9. Cs^+ sorption with time on the Hanford sediment at 10°C or 50°C from 0.1 M NaOH in 1 M $NaNO_3$ at three different initial aqueous $CsNO_3$ concentrations a) 2.1×10^{-9} M, b) 1.3×10^{-7} M, and c) 4.5×10^{-5} M; the horizontal lines are model simulations for Cs sorption at 112-d based on K_c values corrected for enthalpy effects (10°C dashed line; 50°C solid line).

cations (Cs, Rb) and divalent cations (Ca, Sr), Dyer and Faghihian (1998) measured a small (<2%) but significant $Na^+ \rightarrow Cs^+$ exchange component for natrolite over a two week period that suggested a slow exchange process. If the tetranatrolite observed in this study exhibited similar exchange kinetics it would not have been interrogated during the short-term exchange studies.

Table 3. Multiple site model parameters for Na-Cs exchange on the Hanford sediment with K_c values corrected for the influence of temperature[a].

Temperature (°C)	Selectivity coefficient		Site concentration (eq/g)	
	Log K_c(I)	Log K_c(II)	FES[b]	Planar[b]
10[c]	7.57	2.78	2.55×10^{-8}	3.08×10^{-5}
50[c]	6.51	2.08	2.51×10^{-8}	6.73×10^{-5}
10[c]	7.26	2.33	3.45×10^{-8}	4.26×10^{-5}
50[c]	6.32	2.16	3.45×10^{-8}	4.26×10^{-5}

[d] Values for log K_c (I) and (II) are from Zachara et al. (2002a) measured at 30°C (Table 2).
[a] Correction estimates based on Liu et al. (2003).
[b] frayed edge sites (FES) and the basal plane sites (Planar) represent the cation exchange complex in the multiple site model.
[c] Values for log K_c (I) and (II) are based on selectivity coefficients measured at 25°C (Table 2).

Assuming that at 50°C the Si dissolution rate was equal to tetranatrolite precipitation rate and reasonably constant (at about 3.27×10^{-5} mol/L/h/g), a maximum of 7.5×10^{-4} moles (0.28 g) of tetranatrolite would have been precipitated over 105 days. At a minimum, about 0.03 g of tetranatrolite precipitated, based on the estimate that about 1% by weight was required to detect a neoform by the XRD technique used. The exchangeable Na^+ associated with this range in tetranatrolite mass would be 1.5×10^{-3} moles to 1.6×10^{-4} moles. During the 105-d period at 50°C, the sediment sorbed, at the highest density, 3.47×10^{-7} moles of Cs^+, which would displace about 0.23% of tetranatrolite exchangeable Na assuming the minimum mass precipitated.

We surmise that Cs^+ sorption during base attack by 0.1 M NaOH at 50°C, was dominated by ion exchange with the phyllosilicates particularly at the lower Cs^+ adsorption densities, and Cs^+ ion exchange was not greatly affected. At higher Cs^+ adsorption densities, planar phyllosilicates sites initially dominated Cs^+ exchange, but tetranatrolite $Na \rightarrow Cs$ exchange accounted for the time dependent sorption of Cs^+, and the ion exchange model's under prediction of the 112-d Cs^+ surface density.

3.6. Cs^+ Sorption During Base Attack by 1 M or 3 M NaOH and 1.0 M $NaNO_3$ at 50°C.

Cs^+ sorption increased over time with exposure to 1 M NaOH in a similar manner to 0.1 M NaOH (Fig. 10a, b, c). At the lower adsorption densities (Fig. 10a, b) Cs^+ sorption increased sharply during the initial 7 d, and over the following 105 d increased by about the same percentage as that observed at 0.1 M NaOH (3–5%). Unlike the 0.1 M NaOH system, however, the lag, or static, period at the highest adsorption density in 0.1 M NaOH (Fig. 9c) was not evident at 1 M NaOH (Fig. 10c). At the lowest Cs^+ adsorption density (Fig. 10a) time dependent Cs^+ sorption was constant or slightly decreased between 14 d and 56 d, and then increased from 56 d to 112 d.

The slightly convex nature of Cs^+ sorption time profile in 1 M NaOH (Fig. 10a) was more pronounced at 3 M NaOH, and was observed at all Cs^+ adsorption densities (Fig. 10a, b, c). All three Cs^+ concentrations showed an immediate increase in Cs^+ adsorp-

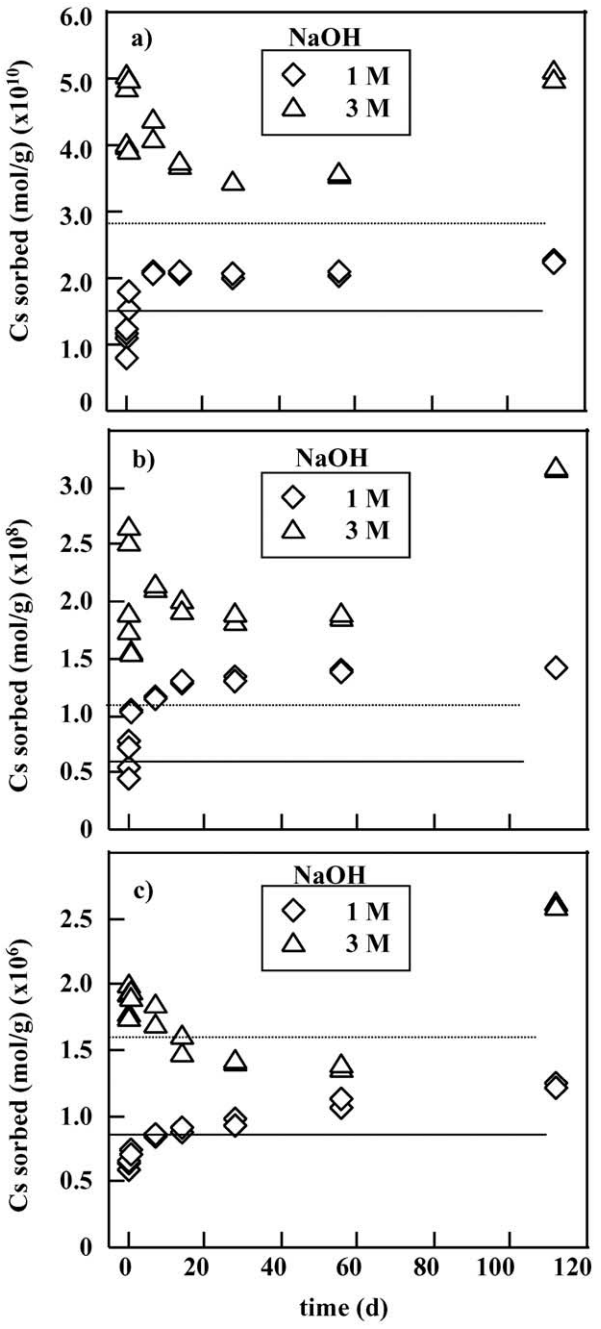

Fig. 10. Cs^+ sorption with time on the Hanford sediment at 50°C from 1 M, or 3 M NaOH in 1 M $NaNO_3$ at different initial aqueous $CsNO_3$ concentrations a) 6.1×10^{-9} M, or 1.3×10^{-8} M at 1 M $NaNO_3$, or 3 M NaOH, respectively, b) 4.0×10^{-7} M, or 8.8×10^{-7} M at 1 M $NaNO_3$, or 3 M NaOH, respectively, and c) 1.3×10^{-4} M, or 3.0×10^{-4} M at 1 M $NaNO_3$, or 3 M NaOH, respectively; solid lines represent Cs^+ sorption to pristine sediment at 30°C in 1 M $NaNO_3$ at initial $[Cs]_{aq}$ used in 1 M base experiments, and the dashed lines represent Cs^+ sorption to pristine sediment at 30°C in 1 M $NaNO_3$ at initial $[Cs]_{aq}$ used in 3 M base experiments.

tion when contacted with base that began to decrease after 24 h. This decrease continued for approximately 40 days; the percentage decrease correlated with adsorption density: 10^{-10} mol/g (23%) $>10^{-8}$ mol/g (17%) $>10^{-6}$ mol/g (10%).

For comparative purposes, model simulations were performed for Cs^+ adsorption to the pristine Hanford sediment at 30°C, with the initial $[Cs^+]_{aq}$ used for each NaOH concentration and 1 M $NaNO_3$; the results are plotted in Figure 10a, b, c as solid (1 M NaOH) and dashed lines (3 M NaOH). Because of enthalpy considerations, greater competition for exchange sites from $[Na^+]_{aq}$ ($[Na]_{total}$ = 2 M and 4 M for 1 and 3 M base treatments, respectively), and clay-sized fraction dissolution (section 3.3), Cs^+ sorption should have been greater on the pristine sediment for an equivalent sorption time. At 1 M NaOH, Cs^+ sorption rapidly increased beyond that estimated for pristine sediment (Fig. 10a, b, c); likewise, at 3 M NaOH only at the highest Cs^+ adsorption density was this condition temporally approximated (Fig. 10c). If, as hypothesized, secondary mineral precipitation (section 3.1, Fig. 3b) did not occur during the initial 24 h, excess Cs^+ adsorption beyond that expected for the pristine sediment was probably the result of base attack on the mica fraction of the sediment via both layer (delamination) and edge weathering (Fanning et al., 1989 and references therein).

Beyond 24 h, base attack resulted in substantial dissolution of the clay fraction phyllosilicates (Fig. 5), and precipitation of $Na_{14}Al_{12}Si_{13}O_{51}\cdot6H_2O$. While the effect of 1 M base on the population and selectivity of high-energy exchange sites is not known, the time-variant sorption behavior of Cs^+ (Fig. 10a, b, c) suggested that the CEC, and primarily the concentration of low affinity exchange sites on silt and sand-sized mica particles, did increase over time. The increase in Cs^+ adsorption observed at the highest adsorption density was probably the result of mica delamination, which in conjunction with precipitation of the $Na_{14}Al_{12}Si_{13}O_{51}\cdot6H_2O$ could generate a greater Cs^+ adsorption potential.

While the decrease in adsorption densities observed between 3 and 40 days in 3 M NaOH may be attributed to the dissolution of the clay fraction phyllosilicates (Fig. 6), the reasons for the increase beyond 40 days was not clear. The formation of $Na_{14}Al_{12}Si_{13}O_{51}\cdot6H_2O$, and its apparent mass increase coincident with dissolution of the sediments clay-sized phyllosilicates suggested that $Na_{14}Al_{12}Si_{13}O_{51}\cdot6H_2O$ was responsible for the late stage increase in adsorption density. Ultimately, however, we could not determine if the neoform influenced Cs^+ adsorption, and if it did, whether uptake occurred through an exchange process or a precipitation/ripening process.

In a similar study, exposure of kaolinite to simulated Cs^+ containing HLW resulted in the precipitation of a zeolite (Alchabalite), nitrate-sodalite, and NO_3-cancrinite (Chorover et al., 2003). Accumulation of Cs with the precipitates was coupled to crystal growth and ripening of the neoforms, and the amount of desorbable (exchangeable) Cs^+ by an unbuffered $Mg(NO_3)_2$, while always low, decreased with reaction time (Chorover et al., 2003). Similarly, reaction between simulated HLW and Hanford sediment produced analcime (a zeolite) after 7 days at 200°C and a 1:1 soil to solution ratio, while at 90°C and 1:10 soil to solution ratio cancrinite formed the predominant reaction product (Nyman et al., 2000). While both of these secondary minerals incorporated Cs^+, the analcime sequestered as much as 4 times that of canrinite.

Because all size fractions of the Hanford sediment contain mica, an alternative explanation is that larger mica grain weathering could qualitatively account for the Cs^+ behavior. At the higher base concentrations, the data suggest that the clay-sized fraction

may have only a minor effect on Cs^+ adsorption. At present, however, there is no way to separate these competing hypotheses. What is clear from the batch reactor studies is that, even at high NaOH concentrations, base-induced dissolution of the Hanford sediment did not adversely influence the sorption of Cs^+. Rather, by 112 days, Cs^+ sorption increased at all initial Cs^+ concentrations compared to sorption on pristine sediments.

3.7. Implications of Base Dissolution for HLW Cs^+ Migration in the Subsurface

A slant borehole was drilled in 2001, beneath the SX-108 tank at Hanford that leaked 380 kL of caustic, saline self-boiling REDOX HLW in 1969 (Serne and Burke, 1997; Jones et al., 2000; Zachara et al., 2002, 2001; Serne et al., 2002a). The REDOX waste was estimated to contain 5.25 M free OH^-, and >10 M $NaNO_3$ at a temperature of 100°C (+). The first sediment core sample that was affected by the HLW plume was about 4.3 m below the tank bottom. Examination of the cored material with depth delineated three important observations: i) the high concentration of Na^+ in the HLW displaced exchangeable cations (Ca^{2+}, Mg^{2+}, K^+) ahead of the body of the waste plume; ii) evidence of base attack, and secondary precipitation on sediment mineral phases were observed to about 10 m below the tank bottom; and iii) base attack intensity was greatest near the tank (McKinley et al., 2001; Zachara et al., 2001; Serne et al., 2002a).

SEM micrographs of borehole sediment revealed that micas just below the tank bottom (4.3 m) were pervasively altered (edges dulled, and curled, crenulated surfaces) with copious secondary precipitates (McKinley et al., 2001). Secondary precipitates on quartz and feldspar grains from the core exhibited a cruciate morphology and Na-Al-Si-O composition similar to those found in the current studies at higher base concentrations (McKinley et al., 2001). With depth, mica alteration and evidence of secondary precipitates diminished, and below 10 m there was no evidence of base attack; mica flakes were sharp-edged with little surface or edge precipitates. Clearly, the alteration/precipitation depth profile reflects base neutralization by mineral dissolution and precipitation reactions and probably recarbonization.

McKinley et al. (2001), found evidence of secondary smectites in the cored materials most altered by base attack. Secondary smectite formation either through a transformation mechanism (via biotite) or as a precipitation reaction could occur under the chemical, and temperature conditions induced by the leaked HLW fluids (Borchardt, 1989 and references therein). Unlike the present study, which observed only $Na_{14}Al_{12}Si_{13}O_{51}{\cdot}6H_2O$ as the primary precipitate after 112-d of reaction with 1 M and 3 M NaOH, the cored sediments have been in ground for almost 40 years at temperatures of 70°C to 100°C, and the pH has been reduced to more natural levels (9.5 to 7.9). The formation of Na-Al-Si-O composition solids observed in the current study and remnants of similar materials observed under the SX-108 tank may indicate that the secondary precipitates observed here are the first stages in a reaction sequence. Autoradiography analysis of individual radioactive particles from the SX-108 borehole found ^{137}Cs activity associated with minute secondary precipitates with chemical composition (Na-Al-Si-O) and morphology consistent with neoforms found in the current study (McKinley et al., 2001).

As in earlier studies with the Hanford sediment (Zachara et al., 2002; Liu et al., 2003a, b), Cs^+ adsorption in the present study is seen as a cation exchange process whose selectivity varies with Cs^+ adsorption density. Unlike earlier work with this sediment, however, a series of reactions occur with base contact that is concomitant/sequential with the Cs^+ exchange reaction. The base-driven reactions alter the Cs^+ exchange complex, but, surprisingly, do not adversely impact Cs^+ sorption. Despite the dissolution of clay-sized phyllosilicates at high base concentrations, Cs^+ adsorption is greater than that predicted for pristine sediment. A number of factors (e.g., rock:water ratio, temperature, solution composition, etc.) influence the precipitation of secondary phase precipitation (amount, mineralogy) after sediment exposure to high base solutions. The neoforms observed to date (zeolites, feldpathoids) exhibit small potential to sorb Cs^+. This small sorption potential, coupled with the fairly unique mica distribution and quantity across all size-fractions in the Hanford sediment, appears to mitigate the impact of base dissolution on Cs^+ sorption.

The similarities between laboratory reacted sediment, and those retrieved from the vasdose zone in Hanford's high level waste tank farms suggests that base reactions will not significantly effect the retardation of Cs^+ in these sediments. The results reported here and those of Zachara et al. (2002) and Liu et al. (2003a, b), indicate that high Na concentrations and elevated temperature, not base attack, are the major factors causing any expedited Cs^+ migration beneath leaked HLW tanks.

Acknowledgments—Research was supported by the Environmental Management Sciences Program (EMSP) and the Hanford Remediation and Closure Science Project. Pacific Northwest National Laboratory is operated for the DOE by Battelle Memorial Institute under Contract DE-AC06-76RLO 1830.

Associate editor: K. L. Nagy

REFERENCES

Amrhein C., Haghnia G. H., Kim T. S., Mosher P. A., Gagajena R. C., Amaanios T., and De La Torre L. (1996) Synthesis and properties of zeolites from coal fly ash. *Environ. Sci. Technol.* **30,** 735–742.

Babcock K. L. and Schultz R. K. (1970) Isotopic and conventional determination of exchangeable sodium percentage of soil in relation to plant growth. *Soil Sci.* **109,** 19–22.

Barnes M. C., Addai-Mensah J., and Gerson A. R. (1999) The mechanism of the sodalite-to-cancrinite phase transformation in the synthetic spent Bayer liquor. *Micropor. Mesopor. Mater.* **31,** 287–302.

Bauer A. and Berger G. (1998) Kaolinite and smectite dissolution rate in high molar KOH solutions at 35° and 80°C. *Appl. Geochem.* **13,** 905–916.

Bauer A., Velde B., and Berger G. (1998) Kaolinite transformation in high molar KOH solutions. *Appl. Geochem.* **13,** 619–629.

Bickmore B. R., Nagy K. L., Young J. S., and Drexler J. W. (2001) Nitrate-cancrinite precipitation on quartz sand in simulated Hanford tanks solutions. *Environ. Sci. Technol.* **35,** 4481–4486.

Borchardt G. (1989) Smectites. In *Minerals In Soil Environments* (eds. J. B. Dixon and S. B. Weed), pp. 675–718. Soil Science Society of America, Madison, WI.

Chermak J. A. (1992) Low temperature experimental investigation of the effect of high pH NaOH solutions on the Opalinus Shale, Switzerland. *Clays Clay Mineral.* **40,** 650–658.

Chermak J. A. (1993) Low temperature experimental investigation of the effect of high pH KOH solutions on the Opalinus Shale, Switzerland. *Clays Clay Mineral.* **41,** 365–372.

Chitra S., Sasidhar P., Lal K. B., and Ahmed J. (1999) The effect of common alkali and alkaline earth metal cations to the sorption of strontium and cesium onto soil. *J. Indust. Pollut. Cont.* **15,** 65–72.

Chorover J., Choi S., Amistadi M. K., Crosson G., and Mueller K. T. (2003) Linking cesium and strontium uptake to kaolinite weathering in simulated tank waste leachate. *Environ. Sci. Technol.* **37,** 2200–2208.

Cremers A., Elsen A., De Preter P., and Maes A. (1988) Quantitative analysis of radiocesium retention in soils. *Nature* **335,** 247–249.

Dyer A. and Faghihian H. (1998) Diffusion in heteroionic zeolites: part 1. Diffusion of water in heteroionic natrolites. *Micropor. Mesopor. Mater.* **21,** 27–38.

Evans D. W., Alberts J. J., and Clark R. A. III (1983) Reversible ion-exchange fixation of cesium-137 leading to mobilization from reservoir sediments. *Geochim. Cosmochim. Acta* **47,** 1041–1049.

Fanning D. S., Keramidas V. Z., and El-Desoky M. A. (1989) Micas. In *Minerals In Soil Environments* (eds. J. B. Dixon and S. B. Weed), pp. 551–624. Soil Science Society of America, Madison, WI.

Francis C. W. and Brinkley F. S. (1976) Preferential adsorption of ^{137}Cs to micaceous minerals in contaminated freshwater sediment. *Nature* **260,** 511–513.

Grütter A., von Gunten H. R., Kohler M., and Rössler E. (1990) Sorption, Desorption and Exchange of Cesium on Glaciofluvial Deposits. *Radiochim. Acta* **50,** 177–184.

Hawkins D. B. (1981) Kinetics of glass dissolution and zeolite formation under hydrothermal conditions. *Clays Clay Mineral.* **29,** 331–340.

Jackson M. L. (1969) Soil Chemical Analysis—Advanced Course. pp.127. Prentice-Hall, Inc., Englewood Cliffs, NJ.

Jones T. E., Watrous R. A., and Maclean G. T. (2000) Inventory estimates for single-shell tank leaks in S and SX tank farms. *RPP-6285 Rev. 0,* CH2MHILL Hanford Group, Inc., Richland, Washington.

Kalinowski B. E. and Schweda P. (1996) Kinetics of muscovite, phlogopite, and biotite dissolution and alteration at pH 1–4, room temperature. *Geochim. Cosmochim. Acta* **60,** 367–385.

Kaviratna H. and Pinnavaia T. J. (1995) Acid hydrolysis of octahedral Mg^{2+} sites in 2:1 layered silicates: An assessment of edge attack and gallery access mechanisms. *Clays Clay Mineral.* **42,** 717–723.

Lee Y., Vogt T., Hriljac J. A., Parise J. B., and Artioli, G. (2002) Pressure induced volume expansion of zeolites in the natrolite family. *J. Am. Chem. Soc.* **124,** 5466–5475.

Lee Y., Kim S. J., and Parise J. B. (2000) Synthesis and crystal structures of gallium- and germanium-variants of the fibrous zeolites with NAT, EDI, and THO structure types. *Micropor. Mesopor. Mater.* **34,** 255–271.

Lin C-F. and Hsi H-C. (1995) Resource recovery of waste fly ash: Synthesis of zeolite-like materials. *Environ. Sci. Technol.* **29,** 1109–1117.

Liu C, Zachara J. M., Qafoku O., and Smith S. C. (2003a) Effect of temperature on Cs^+ sorption and desorption in subsurface sediments at the Hanford Site, USA. *Environ. Sci. Technol.* **37,** 2640–2645.

Liu C., Zachara J. M., Smith S. C., McKinley J. P., and Ainsworth C. C. (2003b) Desorption kinetics of radiocesium from subsurface sediments at Hanford site, USA. *Geochim. Cosmochim. Acta* **67,** 2893–2912.

Ma W., Brown P. W., and Komarneni S. (1998) Characterization and cation exchange properties of zeolite synthesized from fly ashes. *J. Mater. Res.* **13,** 3–7.

Maes A. and Cremers A. (1986) Highly selective ion exchange in clay minerals and zeolites. In *Geochemical Processes at Mineral Surfaces* pp. 254–295. ACS Symposium Series 323, American Chemical Society, Washington, D.C.

Malmström M. and Banwart S. (1997) Biotite dissolution at 25°C: The pH dependence of dissolution rate and stoichiometry. *Geochim. Cosmochim. Acta* **61,** 2779–2799.

McKinley J. P., Zachara J. M., Gassman P. L., Ainsworth C. C., Arey B., McKinley S., Schaef H. T., Smith S. C., Kimberling J., Bish D. L., Chipera S. J., and Snow P. (2001) S-SX Site Mineralogy. In *Appendix D: Digest of S&T Program Evaluations, RPP-7884* (ed. A. J. Knepp) pp. D10–D35. CH2M HILL, Group Inc., Richland.

Ming D. W. and Mumpton F. A. (1989) Zeolites in soils. In *Minerals In Soil Environments* (eds. J. B. Dixon and S. B. Weed), pp. 675–718. Soil Science Society of America, Madison, WI.

Nagy K. L. (1995) Dissolution and precipitation kinetics of sheet silicates. In *Chemical Weathering Rates of Silicate Minerals*, Reviews in Mineralogy, Vol. 31, pp. 173–225. Mineralogical Society of America, Washington, D.C.

Nyman M., Krumhansl J. K., Zhang P., Anderson H., and Nenoff T. M. (2000) Chemical evolution of leaked high-level liquid wastes in Hanford soils. In *Scientific Basis for Nuclear Waste Management XXIII* (eds. R. W. Smith and D. W. Shoesmith) Vol. 608, pp. 225–230. Materials Research Society Symposium Proceedings.

Qafoku N. P., Ainsworth C. C., Szecsody J. E., and Qafoku O. S. (2003a) Aluminum effect on dissolution and precipitation under hyperalkaline conditions: I. Liqiud phase transformations. *J. Environ. Qual.* **32,** 2354–2363.

Qafoku N. P., Ainsworth C. C., Szecsody J. E., Bish D. L., Young J. S., McCready D. E., and Qafoku O. S. (2003b) Aluminum effect on dissolution and precipitation under hyperalkaline conditions: I. Solid phase transformations. *J. Environ. Qual.* **32,** 2364–2372.

Rai R., Felmy A. R., Juracich S. P., and Rao L. (1995) Estimating the hydrogen ion concentration in concentrated NaCl and Na_2SO_4 electrolytes. SAND94-1949, Sandia National Laboratory, Albuquerque, NM.

Samson S. D., Nagy K. L., and Cotton W. B. III. (2005) Transient and quasi-steady-state dissolution of biotite at 22–25°C in high pH, sodium, nitrate, and aluminate solutions. *Geochim. Cosmochim. Acta* **69,** 399–413.

Serne R. J., Schaef H. T., Last G. V., Lanigan D. C., Lindenmeier C. W., Clayton R. E., LeGore V. L., O'Hara M. J., Brown C. F., Orr R. D., Kutnyakov I. V., Wilson T. C., Burke D. B., Williams B. A., and Bjornstad B. N. (2002a) Geologic and geochemical data collected from vadose zone sediments from the slant borehole under SX-108 in the S/SX waste management area and preliminary interpretations, *PNNL-2001-4*, Pacific Northwest National Laboratory, Richland, Washington.

Serne R. J., Bjornstad B. N., Schaef H. T., Williams B. A., Lanigan D. C., Horton D. G., Clayton R. E., Mitroshkov A. V., Legore V. L., O'Hara M. J., Brown C. F., Parker K. E., Kutnyakov I. V., Serne J. N., Last G. V., Smith S. C., Lindenmeier C. W., Zachara J. M., and Burke D. (2002b) Characterization of vadose zone sediment: uncontaminated RCRA borehole core samples and composite samples. *PNNL-13757-1*, Pacific Northwest National Laboratory, Richland, WA.

Serne R. J. and Burke D. S. (1997). Chemical information on tank supernatants, Cs adsorption from tank liquids onto Hanford sediments, and field observations of Cs migration from past tank leaks. *PNNL-11495*, Pacific Northwest National Laboratory, Richland, WA.

Steefel C. I., Carrol S., Zhao P., and Roberts S. (2003) Cesium migration in Hanford sediment: a multisite cation exchange model based on laboratory transport experiments. *J. Contam. Hydrol.* **67,** 219–246.

Trotignon L. and Turpault M-P. (1992) The dissolution kinetics of biotite in dilute HNO_3 at 24°C. In *Proc. 7th International Symposium on Water-Rock Interactions-WRI-7* (eds. Y. K. Kharaka and A. S. Maest), pp. 847–850. Balkema, Rotterdam.

Turpault M-P. and Trotignon L. (1994) The dissolution of biotite single crystals in dilute HNO_3 at 24 C: Evidence of an anisotropic corrosion process of micas in acidic solutions. *Geochim. Cosmochim. Acta* **58,** 2761–2775.

Wauters J., Vidal M., Elsen A., and Cremers A. (1996a) Prediction of solid/liquid distribution coefficients of radiocaesium in soils and sediments. Part two: A new procedure for solid phase speciation of radiocaesium. *Appl. Geochem.* **11,** 595–599.

Wauters J., Elsen A., and Cremers A. (1996b) Prediction of solid/liquid distribution coefficients of radioCaesium in soils and sediments. Part three: A quantitative test of a K_D predictive equation. *Appl. Geochem.* **11,** 601–603.

Zachara J. M., Smith S. C., Liu C., McKinley J. P., Serne R. J., and Gassman P. L. (2002) Sorption of Cs+ to micaceous subsurface sediments from the Hanford site, USA. *Geochim. Cosmochim. Acta* **66,** 193–211.

Zachara J. M., Liu C., Smith S. C., and Ainsworth C. C. (2001) Adsorption of Cs in WMA S-SX sediments in the presence of high salt and high base. In *Appendix D: Digest of S&T Program Evaluations, RPP-7884* (ed. A. J. Knepp) CH2M HILL, Group Inc., Richland, WA.